Observation of Excited Quadrupole-Bound States in Cold Anions

Guo-Zhu Zhu, Yuan Liu, and Lai-Sheng Wang*
Department of Chemistry, Brown University, Providence, Rhode Island 02912, USA
(Received 5 May 2017; published 11 July 2017)

We report the first observation of an excited quadrupole-bound state (QBS) in an anion. High-resolution photoelectron imaging of cryogenically cooled 4-cyanophenoxide ($4CP^-$) anions yields an electron detachment threshold of 24 927 cm^{-1}. The photodetachment spectrum reveals a resonant transition 20 cm^{-1} below the detachment threshold, which is attributed to an excited QBS of $4CP^-$ because neutral 4CP has a large quadrupole moment with a negligible dipole moment. The QBS is confirmed by observation of seventeen above-threshold resonances due to autodetachment from vibrational levels of the QBS.

DOI: 10.1103/PhysRevLett.119.023002

A dipolar molecule can bind an electron in a diffuse orbital, which is dominated by the long-range charge-dipole attractive potential scaled as $1/r^2$ [1–3]. Such dipole-bound states (DBSs) play important roles in electron-molecule interactions and are considered to be the "doorway" to the formation of valence-bound anions [4–6]. Fermi and Teller first predicted a critical dipole moment of 1.625 D for a point dipole to bind an electron [7]. Many subsequent theoretical [8–10] and experimental [11,12] studies have shown that the practical minimum dipole moment is 2.5 D to form dipole-bound anions, which have been produced via Rydberg electron transfer (RET) [11–13] and electron attachment [14,15] and investigated by field detachment and photoelectron spectroscopy (PES). Stable anions with dipolar cores can possess excited DBSs just below the electron detachment threshold. Excited DBSs of valence-bound anions were first observed as resonances in photodetachment cross sections [16] and studied via rotational and vibrational autodetachment [17–19]. Vibrationally induced autodetachment from selected vibrational levels of an excited DBS, yielding highly non-Franck-Condon resonant PE spectra, has also been investigated recently [20–23].

With vanishing dipole moments, but strong quadrupole moments, neutral molecules can form quadrupole-bound anions, in which the long-range charge-quadrupole attractive potential ($\sim 1/r^3$) dominates [1,3,24,25]. Jordan and Liebman first suggested the rhombic $(BeO)_2^-$ cluster as a quadrupole-bound anion [26]. This cluster and the similar $(MgO)_2^-$ cluster studied by PES [27] have relatively high electron binding energies and should probably be considered as valence-bound anions [3]. In addition, the rhombic alkali-halide dimers and a series of complex organic molecules with vanishing dipole moments but large quadrupole moments have also been proposed to form quadrupole-bound anions [28–30]. Experimental studies of electron binding to quadrupolar molecules have been scarce. The CS_2^- anion was first observed via RET and was suggested to be a possible quadrupole-bound anion [31,32]. The formamide dimer and the *para*-dinitrobenzene anions formed via RET were suggested to be quadrupole-bound anions [33,34]. A more conclusive example of a quadrupole-bound anion was from RET to the *trans*-succinonitrile [35,36]. A valence-bound anion with a nonpolar core may possess excited quadrupole-bound state (QBS) just below the electron detachment threshold, if the neutral core possesses a large quadrupole moment. However, such an excited QBS has not been observed heretofore.

Here we report the first observation of an excited QBS in the 4-cyanophenoxide anion ($4CP^-$) cryogenically cooled in an ion trap. The neutral 4CP radical has a very small dipole moment of 0.3 D (see inset of Fig. 1), which is insufficient to form a DBS. Its large quadrupole moment (traceless quadrupole moment: $Q_{xx} = 5.4$, $Q_{yy} = 15.1$, $Q_{zz} = -20.5$ D Å) suggests that it may be a good candidate to search for excited QBS. The experiment was carried out on an electrospray-PES apparatus [37], equipped with a cryogenically cooled Paul trap [38] and a high-resolution PE imaging system [39]. A more detailed experimental procedure is provided in the Supplemental Material [40]. Figure 1 shows the non-resonant PE images and spectra of $4CP^-$ at three photon energies. The first intense peak, labeled as 0_0^0, denotes the detachment transition from the vibrational ground state of $4CP^-$ to that of neutral 4CP, representing the electron affinity of 4CP or the electron detachment threshold of $4CP^-$. The spectrum in Fig. 1(a), with a photon energy slightly above the detachment threshold, gives the best resolved 0_0^0 peak with a width of 11 cm^{-1} mainly due to rotational broadening, yielding an accurate electron affinity for 4CP as 24 927 $\pm$ 5 cm^{-1}. At higher photon energies, numerous vibrational peaks, labeled as *A*-*J*, are resolved for the ground electronic state of 4CP. The strongest vibrational peak *B* corresponds to the most Franck-Condon-active mode. To better resolve peak *B*, we tuned the detachment laser to be just above the binding energy of peak *B* at 393.57 nm, resolving an additional weak peak *C*. The intensity of peak *B* is significantly enhanced due to the threshold effect. The

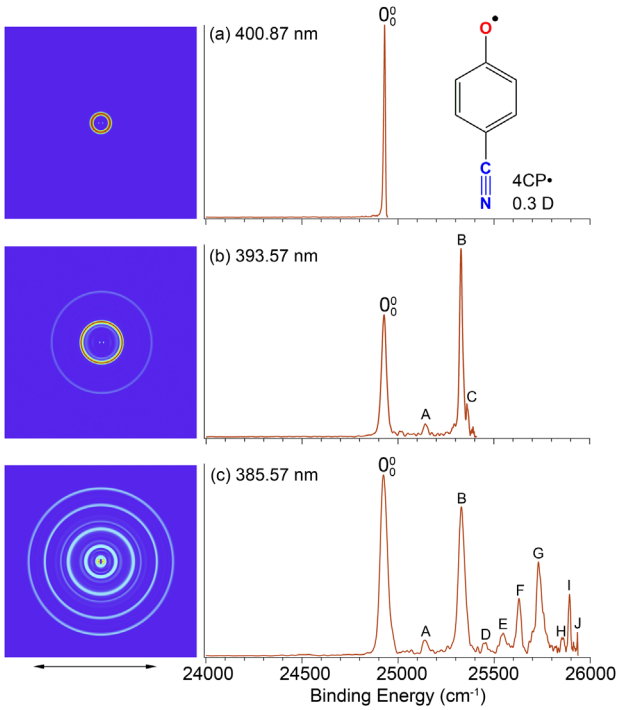

FIG. 1. Nonresonant photoelectron images and spectra of $4CP^-$ at (a) 400.87, (b) 393.57, and (c) 385.57 nm. The double arrow below the images indicates the direction of the laser polarization. The structure and dipole moment of neutral 4CP are shown in the inset of (a).

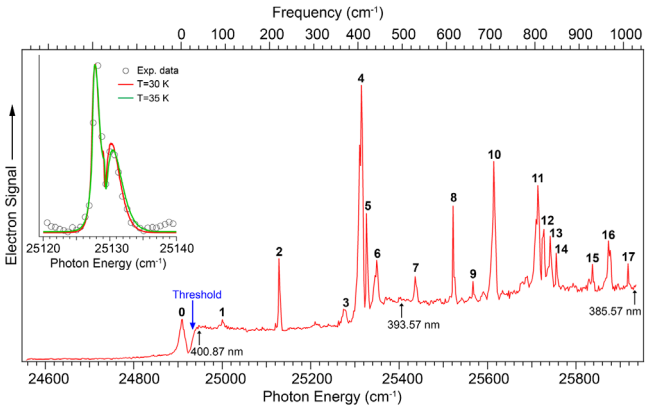

FIG. 2. Photodetachment spectrum of $4CP^-$ by measuring the total electron yield as a function of photon energy across the detachment threshold. The blue arrow at 24 927 cm^{-1} indicates the detachment threshold of $4CP^-$. The three black arrows indicate the detachment photon energies used for the nonresonant PE spectra in Fig. 1. The peaks 1–17 are due to autodetachment from QBS vibrational levels of $4CP^-$, while peak 0 below threshold represents the vibrational ground state of the QBS and is from resonant two-photon processes. The inset shows a high-resolution scan of peak 2, revealing the rotational profile, along with rotational simulations at two temperatures (see Supplemental Material [40]).

electron binding energies of all the observed vibrational peaks, their shifts from peak 0_0^0, and their assignments are summarized in Table S1 [40].

To search for possible QBSs, we measured the photodetachment spectrum of $4CP^-$ by monitoring the total electron yield while scanning the dye laser across the detachment threshold (Fig. 2). The blue arrow at 24 927 cm^{-1} indicates the detachment threshold, consistent with the PE spectra in Fig. 1. The three black arrows indicate the detachment wavelengths used in the nonresonant PE images in Fig. 1. Below threshold, one broad peak, labeled as 0, is observed due to two-photon processes. Because $4CP^-$ cannot support DBSs, this below-threshold peak should be due to the vibrational ground state of the putative QBS, because no other peaks were observed below peak 0. This peak is 20 cm^{-1} below the detachment threshold, suggesting the weakly bound nature of the electron in the QBS relative to the detachment continuum. The continuous signals above threshold represent nonresonant photodetachment signals. Seventeen above-threshold peaks are observed, due to autodetachment from excited vibrational levels of the QBS. The inset shows the simulation of the rotational profile for peak 2 at a high resolution scan, yielding a rotational temperature of 30–35 K, consistent with previous estimates [21,44]. See the Supplemental Material for details of the rotational simulation [40]. The top scale is relative to the vibrational ground state of the QBS. The corresponding photon energies, shifts from peak 0, and assignments of the photodetachment spectrum are given in Table S2 [40].

The local dipoles of the two polar centers (–CN and C-O) in the neutral planar 4CP radical have opposite directions, resulting in a small dipole moment of 0.3 D but a large quadrupole moment. Hence, the dominating potential that binds the electron in the excited state of $4CP^-$ should be between the quadrupole moment and the electron. This interaction is scaled as $1/r^3$, much weaker than the electron-dipole interaction in DBSs. The peak 0 observed in Fig. 2 gives rise to a small binding energy of 20 cm^{-1} for the QBS of $4CP^-$. Thus, any vibrational excitation of the QBS would be above the detachment threshold and can lead to vibrationally induced autodetachment via vibrational to electronic energy transfer or vibronic coupling. The electron in the excited QBS is expected to be in a highly diffuse orbital with little effect on the structure of the neutral core. This is confirmed by the similarity of the observed vibrational peaks in the photodetachment spectrum in Fig. 2 and those in the nonresonant PE spectrum in Fig. 1(c). A direct comparison is presented in Fig. S1, where the 385.57 nm PE spectrum is overlaid onto the photodetachment spectrum in the same energy scale by aligning the peak 0_0^0 in the PE spectrum and the peak 0 of the photodetachment spectrum. All the major vibrational peaks and their relative intensities agree with each other in the two spectra, except that the photodetachment spectrum has higher resolution. This resemblance provides strong evidence for the weakly bound nature of the excess electron

in the QBS, which has little effect to the neutral core, just as that observed for DBSs [20–23]. Hence, the photodetachment spectrum of the QBS can be used to yield more accurate vibrational information for the neutral radical.

By tuning the dye laser wavelength to the above-threshold peaks, we have obtained seventeen high-resolution resonantly enhanced PE images and spectra. Six of these spectra are shown in Fig. 3 and the remaining eleven spectra are given in Fig. S2 [40]. These resonant PE spectra consist of contributions from two different detachment processes: (i) nonresonant detachment represented by the baseline in Fig. 2 (such as the spectra in Fig. 1), and (ii) the much stronger resonant autodetachment signal represented by the above-threshold peaks. The latter involves two steps, i.e., resonant excitation to a vibrational level of the QBS, followed by transfer of vibrational energies to the weakly bound electron to induce detachment. The vibrationally induced autodetachment from DBSs generally obeys the $\Delta\nu = -1$ propensity rule under the harmonic-oscillator approximation [45,46] and yields highly non-Franck-Condon PE spectra [20–23]. This propensity rule is expected to hold true for vibrational autodetachment from the QBS due to the even more weakly bound nature of the QBS electron. The six spectra in Fig. 3 show autodetachment involving single vibrational modes of the QBS, while the eleven spectra in Fig. S2 represent excitations to combinational and overlapping vibrational levels of the QBS. The enhanced vibrational levels (in bold face), the detachment laser wavelengths, the assigned vibrational levels of the QBS, and the corresponding peak number (in parentheses) used in Fig. 2 are given in each spectrum. Ten new

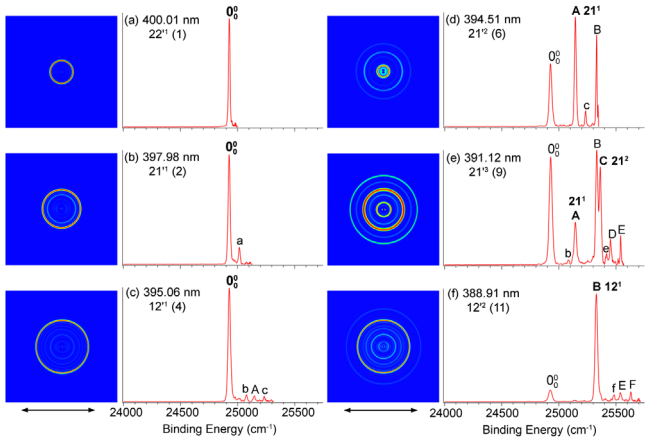

FIG. 3. Resonant photoelectron images and spectra of $4CP^-$ at six different detachment wavelengths, corresponding to excitations to vibrational levels involving single vibrational modes of the QBS followed by autodetachment via vibronic coupling. The QBS vibrational levels and the peak number (in parentheses) used in Fig. 2 are given. The peaks labeled in bold face indicate the autodetachment-enhanced final neutral vibrational levels. The double arrows below the images represent the direction of the laser polarization.

vibrational peaks, labeled as *a*-*j*, are observed in the resonant PE spectra and are also listed in Table S1 [40].

To understand the vibrational peaks in Figs. 1 and 2, we calculated the vibrational frequencies of neutral 4CP at the B3LYP/6-311 + +$G(d, p)$ level (Table S3 [40]). The thirty-three normal modes are shown in Fig. S3 [40]. The calculated frequencies are unscaled and agree well with the observed frequencies for most vibrational modes. Because both $4CP^-$ and 4CP have C_{2v} symmetry, only modes with A_1 symmetry are allowed in principle. Peaks *B* and *G* form a vibrational progression for the most Franck-Condon-active mode ν_{12} (A_1), which is an in-plane $N\ldots O$ stretching mode (Fig. S3). The very weak peaks *A* and *C* correspond to a vibrational progression of the ν_{21} (B_1) mode, which is an out-of-plane bending mode (Fig. S3). The assignments of all the observed peaks are given in Table S1 [40] by using the calculated vibrational frequencies and the resonant PE spectra.

According to the $\Delta\nu = -1$ propensity rule for vibrationally induced autodetachment, excitation to the *n*th vibrational level of a given mode (ν_x^n) of the QBS autodetaches to the $(n-1)$th level of the same neutral mode (ν_x^{n-1}) with one vibrational quantum transferred to the QBS electron. The corresponding ν_x^{n-1} vibrational peak will be enhanced relative to that in the nonresonant PE spectrum, giving rise to highly non-Franck-Condon PE spectra. Figures 3(a)–3(c) show significant enhancement of peak 0_0^0, indicating autodetachment from the fundamental vibrational level of different modes ($\nu_x'^1$) of the QBS. The photon energies used for the spectra in Figs. 3(a)–3(c) correspond to excitations to vibrational levels $22'^1$, $21'^1$, and $12'^1$ of the QBS, respectively. In Figs. 3(d) and 3(f), peaks *A* and *B*, corresponding to vibrational level 21^1 and 12^1 of 4CP, respectively, are greatly enhanced in comparison to the intensity of peak 0_0^0 in the nonresonant PE spectra. These are due to excitations to the QBS vibrational levels of $21'^2$ and $12'^2$, respectively, followed by $\Delta\nu = -1$ autodetachment. Both peaks *A* (21^1) and *C* (21^2) in Fig. 3(e) are enhanced. The photon energy used for the spectrum in Fig. 3(e) corresponds to excitation to the $21'^3$ vibrational level of the QBS. Hence, the enhancement of peak *A* is a result of transferring two vibrational quanta to the QBS electron (i.e., $\Delta\nu = -2$), which suggests a large anharmonicity in the ν_{21}' (B_1) mode [45]. Figure 4 displays the six vibrational levels of the QBS and their autodetachment processes to the neutral final vibrational states, as revealed in the six resonantly enhanced PE spectra in Fig. 3. In addition, numerous weak peaks *a*-*c*, *e*, and *f* are also observed in Fig. 3. As given in Table S1 [40], the shifts of peaks *a* and *b* relative to peak 0_0^0 are 89 and 155 cm^{-1}, respectively, which correspond to the two lowest frequency modes ν_{22} (B_1) and ν_{33} (B_2) of neutral 4CP (Table S2 [40]). Their appearances in the resonant PE spectra are most likely due to intramolecular electron rescattering, as

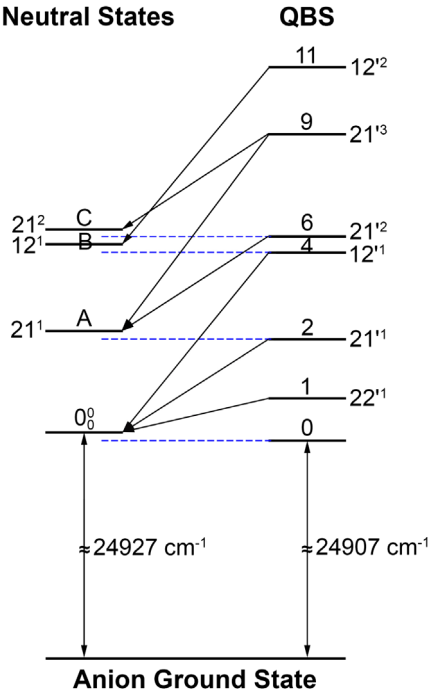

FIG. 4. A schematic energy level diagram for autodetachment from the QBS vibrational levels of $4CP^-$ to the neutral final states of 4CP, corresponding to the six resonant PE spectra shown in Fig. 3. The detachment threshold (24 927 cm^{-1}) of $4CP^-$ and the excitation energy (24 907 cm^{-1}) to the ground vibrational level of the QBS are shown. See Fig. S4 for a more complete energy level diagram for all the seventeen QBS vibrational levels and their autodetachment channels.

observed previously [23]. The assignments of peaks c (33^2), e ($12^1 22^1$), and f (31^1) are based on the calculated frequencies.

The remaining eleven resonant PE spectra (Fig. S2) all involve excitations to combinational or overlapping vibrational levels of the QBS with more complicated autodetachment processes. All spectra can be well understood and assigned similarly using the computed vibrational frequencies and the $\Delta\nu = -1$ autodetachment propensity rule, as presented in the Supplemental Material [40]. All the assignments for the observed vibrational resonances of the QBS are summarized in Table S2 [40]. A more complete energy level diagram for all the seventeen QBS vibrational levels and the observed autodetachment channels are given in Fig. S4. The experimental vibrational frequencies for 4CP are compared with the calculated frequencies in Table S3 [40].

In conclusion, we report the first observation of an excited quadrupole-bound state for cryogenically cooled cyanophenoxide anions, whose neutral core possesses a very small dipole moment but a large quadruple moment [47]. The quadrupole-bound state is found to have a binding energy of 20 cm^{-1} relative to the detachment threshold. Seventeen excited vibrational levels of the QBS are observed as resonances in the photodetachment spectrum. The weakly bound nature of the electron in the QBS is confirmed by the observation of the similarity of the nonresonant PE spectra and the photodetachment spectrum and the $\Delta\nu = -1$ vibrational autodetachment propensity rule in the resonant PE spectra.

The authors gratefully acknowledge the Division of Chemical Sciences, Geosciences, and Biosciences, Office of Basic Energy Sciences of the U.S. Department of Energy for early support of the development of the electrospray-PES facility that made this research possible.

*Lai-Sheng_Wang@brown.edu

[1] R. N. Comptonand N. I. Hammer in *Advances in Gas-Phase Ion Chemistry*, edited by N. Adams and I. Babcock (Elsevier Science, New York, 2001), Vol. 4, p. 257.
[2] K. D. Jordan and F. Wang, Annu. Rev. Phys. Chem. **54**, 367 (2003).
[3] J. Simons, J. Phys. Chem. A **112**, 6401 (2008).
[4] C. Desfrancois, B. Baillon, J. P. Schermann, S. T. Arnold, J. H. Hendricks, and K. H. Bowen, Phys. Rev. Lett. **72**, 48 (1994).
[5] R. N. Compton, J. H. S. Carman, C. Desfrancois, H. Abdoul-Carime, J. P. Schermann, J. H. Hendricks, S. A. Lyapustina, and K. H. Bowen, J. Chem. Phys. **105**, 3472 (1996).
[6] T. Sommerfeld, Phys. Chem. Chem. Phys. **4**, 2511 (2002).
[7] E. Fermi and E. Teller, Phys. Rev. **72**, 399 (1947).
[8] O. H. Crawford, Mol. Phys. **20**, 585 (1971).
[9] W. R. Garrett, Phys. Rev. A **3**, 961 (1971).
[10] J. E. Turner, Am. J. Phys. **45**, 758 (1977).
[11] C. Desfrançois, H. Abdoul-Carime, N. Khelifa, and J. P. Schermann, Phys. Rev. Lett. **73**, 2436 (1994).
[12] C. Desfrançois, H. Abdoul-Carime, and J. P. Scherman, Int. J. Mod. Phys. B **10**, 1339 (1996).
[13] N. I. Hammer, K. Diri, K. D. Jordan, C. Desfrançois, and R. N. Compton, J. Chem. Phys. **119**, 3650 (2003).
[14] J. H. Hendricks, S. A. Lyapustina, H. L. de Clercq, J. T. Snodgrass, and K. H. Bowen, J. Chem. Phys. **104**, 7788 (1996).
[15] A. M. Buytendyk, A. M. Buonaugurio, S. J. Xu, J. M. Nilles, K. H. Bowen, N. Kirnosov, and L. Adamowicz, J. Chem. Phys. **145**, 024301 (2016).
[16] A. H. Zimmerman and J. I. Brauman, J. Chem. Phys. **66**, 5823 (1977).
[17] K. R. Lykke, R. D. Mead, and W. C. Lineberger, Phys. Rev. Lett. **52**, 2221 (1984).
[18] R. D. Mead, K. R. Lykke, W. C. Lineberger, J. Marks, and J. I. Brauman, J. Chem. Phys. **81**, 4883 (1984).
[19] K. Yokoyama, G. W. Leach, J. B. Kim, W. C. Lineberger, A. I. Boldyrev, and M. Gutowski, J. Chem. Phys. **105**, 10706 (1996).
[20] H. T. Liu, C. G. Ning, D. L. Huang, P. D. Dau, and L. S. Wang, Angew. Chem., Int. Ed. Engl. **52**, 8976 (2013).
[21] D. L. Huang, G. Z. Zhu, and L. S. Wang, J. Chem. Phys. **142**, 091103 (2015).
[22] G. Z. Zhu, D. H. Huang, and L. S. Wang, J. Chem. Phys. **147**, 013910 (2017).

[23] D. L. Huang, H. T. Liu, C. G. Ning, P. D. Dau, and L. S. Wang, Chem. Phys. **482**, 374 (2017).
[24] A. Ferron, P. Serra, and S. Kais, J. Chem. Phys. **120**, 8412 (2004).
[25] W. R. Garrett, J. Chem. Phys. **136**, 054116 (2012).
[26] K. D. Jordan and J. F. Liebman, Chem. Phys. Lett. **62**, 143 (1979).
[27] M. Gutowski, P. Skurski, X. Li, and L. S. Wang, Phys. Rev. Lett. **85**, 3145 (2000).
[28] G. L. Gutsev, P. Jena, and R. J. Bartlett, J. Chem. Phys. **111**, 504 (1999).
[29] I. Anusiewicz, P. Skurski, and J. Simons, J. Phys. Chem. A **106**, 10636 (2002).
[30] T. Sommerfeld, K. M. Dreux, and R. Joshi, J. Phys. Chem. A **118**, 7320 (2014).
[31] C. Desfrancois, N. Khelifa, J. P. Schermann, T. Kraft, M. W. Ruf, and H. Hotop, Z. Phys. D **27**, 365 (1993).
[32] R. N. Compton, F. B. Dunning, and P. Nordlander, Chem. Phys. Lett. **253**, 8 (1996).
[33] C. Desfrancois, V. Periquet, S. Carles, J. P. Schermann, and L. Adamowicz, Chem. Phys. **239**, 475 (1998).
[34] C. Desfrancois, V. Periquet, S. A. Lyapustina, T. P. Lippa, D. W. Robinson, K. H. Bowen, H. Nonaka, and R. N. Compton, J. Chem. Phys. **111**, 4569 (1999).
[35] C. Desfrancois, Y. Bouteiller, J. P. Schermann, D. Radisic, S. T. Stokes, K. H. Bowen, N. I. Hammer, and R. N. Compton, Phys. Rev. Lett. **92**, 083003 (2004).
[36] T. Sommerfeld, J. Chem. Phys. **121**, 4097 (2004).
[37] L. S. Wang, J. Chem. Phys. **143**, 040901 (2015).
[38] X. B. Wang and L. S. Wang, Rev. Sci. Instrum. **79**, 073108 (2008).
[39] I. León, Z. Yang, H. T. Liu, and L. S. Wang. Rev. Sci. Instrum. **85**, 083106 (2014).
[40] See Supplemental Material at http://link.aps.org/supplemental/10.1103/PhysRevLett.119.023002 for discussions on experimental details, rotational simulation, autodetachment involving combinational and overlapping vibrational levels, Tables S1-S3, Figs. S1-S4, as well as Ref. [41–43].
[41] G. A. Garcia, L. Nahon, and I. Powis, Rev. Sci. Instrum. **75**, 4989 (2004).
[42] V. Dribinski, A. Ossadtchi, V. A. Mandelshtam, and H. Reisler, Rev. Sci. Instrum. **73**, 2634 (2002).
[43] PGOPHER, A Program for Simulating Rotational, Vibrational and Electronic Spectra, C. M. Western, University of Bristol, http://pgopher.chm.bris.ac.uk.
[44] H. T. Liu, C. G. Ning, D. L. Huang, and L. S. Wang, Angew. Chem. Int. Ed. **53**, 2464 (2014).
[45] R. S. Berry, J. Chem. Phys. **45**, 1228 (1966).
[46] J. Simons, J. Am. Chem. Soc. **103**, 3971 (1981).
[47] Noncovalent correlation bound anions have been predicted to exist computationally for neutral cores without either dipole or quadrupole moments. See, for example, V. K. Voora, L. S. Cederbaum, and K. D. Jordan, J. Phys. Chem. Lett. **4**, 849 (2013); V. K. Voora and K. D. Jordan, J. Phys. Chem. A **118**, 7201 (2014); V. K. Voora and K. D. Jordan, J. Phys. Chem. Lett. **6**, 3994 (2015). Such correlation effects should also play a role in both quadrupole-bound and dipole-bound states.